
**Online measurements of cycloalkanes based on NO⁺ chemical
ionization in proton transfer reaction time of flight mass
spectrometry (PTR-ToF-MS)**

Yubin Chen^{1,2}, Bin Yuan^{1,2,*}, Chaomin Wang³, Sihang Wang^{1,2}, Xianjun He^{1,2},
Caihong Wu^{1,2}, Xin Song^{1,2}, Yibo Huangfu^{1,2}, Xiao-Bing Li^{1,2}, Yijia Liao^{1,2}, Min
Shao^{1,2}

¹ Institute for Environmental and Climate Research, Jinan University, Guangzhou
511443, China

² Guangdong-Hongkong-Macau Joint Laboratory of Collaborative Innovation for
Environmental Quality, Guangzhou 511443, China

³ School of Tourism and Culture, Guangdong Eco-engineering Polytechnic,
Guangzhou 510520, China

*Correspondence to: Bin Yuan (byuan@jnu.edu.cn)

Abstract:

Cycloalkanes are important trace hydrocarbons existing in the atmosphere, and they are considered as a major class of intermediate volatile organic compounds (IVOCs). Laboratory experiments showed that the yields of secondary organic aerosols (SOA) from oxidation of cycloalkanes are relatively higher than acyclic alkanes with the same carbon number. However, measurements of cycloalkanes in the atmosphere are still challenging at present. In this study, we show that online measurements of cycloalkanes can be achieved using proton transfer reaction time-of-flight mass spectrometry with NO^+ chemical ionization (NO^+ PTR-ToF-MS). Cyclic and bicyclic alkanes are ionized with NO^+ via hydride ion transfer leading to major product ions of $\text{C}_n\text{H}_{2n-1}^+$ and $\text{C}_n\text{H}_{2n-3}^+$, respectively. As isomers of cycloalkanes, alkenes ~~undergoes~~undergo association reactions with major product ions of $\text{C}_n\text{H}_{2n}^\bullet(\text{NO})^+$, and concentrations of 1-alkenes and trans-2-alkenes in the atmosphere are usually significantly lower than cycloalkanes (about 25% and <5%, respectively), as ~~the a~~ result inducing little interference to cycloalkanes detection in the atmosphere. Calibration of various cycloalkanes show similar sensitivities, associated with small humidity dependence. Applying this method, cycloalkanes were successfully measured at an urban site in southern China and during a chassis dynamometer study for vehicular emissions. Concentrations of both cyclic and bicyclic alkanes are significant in urban air and vehicular emissions, with comparable cyclic alkanes/acyclic alkanes ratios between urban air and gasoline vehicles. These results ~~demonstrates~~demonstrate that NO^+ PTR-ToF-MS provides a new complementary approach for fast characterization of cycloalkanes in both ambient air and emission sources, which can be helpful to fill the gap in understanding the importance of cycloalkanes in the atmosphere.

1 Introduction

Organic compounds, as important trace components in the atmosphere, are released to the atmosphere from many different natural and anthropogenic sources, which have complicated and diverse chemical compositions (de Gouw, 2005; Goldstein and Galbally, 2007; He et al., 2022). Components and concentration levels of organic compounds ~~affect largely on~~largely affect atmospheric chemistry, atmospheric oxidation capacity, and radiation balance (Monks et al., 2015; Wu et al., 2020), as well as human health (Xing et al., 2018). According effective saturation concentrations (Donahue et al., 2012), organic compounds can be divided into intermediate volatile organic compounds (IVOCs), semi-volatile organic compounds (SVOCs), low volatile organic compounds (LVOCs), and extremely low volatile organic compounds (ELVOCs). Due to high yields of secondary organic aerosol (SOA) (Lim and Ziemann, 2009; Robinson et al., 2007), IVOCs have been proved to be important SOA precursors in urban atmospheres (Tkacik et al., 2012; Zhao et al., 2014).

Many studies showed that higher alkanes (i.e., linear and branched alkanes with 12-20 carbon atoms) to be important chemical components of IVOCs (Li et al., 2019; Zhao et al., 2014). Similar to these acyclic alkanes, cycloalkanes can also account for significant fractions of IVOCs. Cycloalkanes can reach more than 20% of IVOCs concentrations in diesel vehicle exhausts, lubricating oil, and diesel fuels (Alam et al., 2018; Liang et al., 2018; Lou et al., 2019), which are comparable or even higher than linear and branched alkanes. In some oil and gas regions, high concentrations of cycloalkanes were also reported (Aklilu et al., 2018; Gilman et al., 2013; Warneke et al., 2014). More importantly, laboratory studies suggest that SOA yields of cyclic and polycyclic alkanes are significantly higher than linear or branched alkanes with the same carbon number (as high as a factor of 5) (Hunter et al., 2014; Jahn et al., 2021; Li et al., 2021a; Loza et al., 2014; Yee et al., 2013). As the result, cyclic and bicyclic species are shown to be large contributors to SOA formation potential from vehicles (Xu et al., 2020a, b; Zhao et al., 2015; Zhao et al., 2016). Recently, Hu et al. (2022)

proposed that IVOCs contributions to SOA formation in an urban region can increase from 8-20% (acyclic alkanes only) to 17.5-46% if cycloalkanes are considered, signifying the importance of cycloalkanes in SOA formation.

Cycloalkanes are mainly measured using gas chromatography-mass spectrometer/flame ionization detector (GC-MS/FID) and two-dimensional gas chromatography techniques (GC×GC) (Alam et al., 2018; Alam et al., 2016; de Gouw et al., 2017; Liang et al., 2018; Zhao et al., 2016). Based on measurements of gas chromatographic techniques, the signals of unseparated cyclic compounds can be determined. ~~This is done by from~~ subtracting the total signal for each retention time bin according to the series of *n*-alkanes (Zhao et al., 2014; Zhao et al., 2016). The mass of linear alkanes and branched alkanes in each bin is calculated by using the total ion current (TIC) and the fraction of characteristic fragments ($C_4H_9^+$, m/z 57) (Zhao et al., 2014; Zhao et al., 2016). However, this type of quantitative method does not explicitly distinguish individual cycloalkanes, and the determined mass may contain other cyclic compounds, e.g., polycyclic aromatic hydrocarbons and compounds containing oxygen or multifunctional groups (Zhao et al., 2014; Zhao et al., 2015; Zhao et al., 2016). Due to the need for collection and pretreatment of air samples, time resolution of GC-MS techniques is usually in the range of 0.5-1.0 h or above.

Proton transfer reaction mass spectrometer (PTR-MS) using hydronium ions (H_3O^+) as the reagent ion, is capable for measuring many organic compounds with high response time and sensitivity (de Gouw and Warneke, 2007; Yuan et al., 2017). However, detection of alkanes and cycloalkanes using PTR-MS with H_3O^+ ionization is challenging, as usually only a series of fragment ions ($C_nH_{2n+1}^+$, $C_nH_{2n-1}^+$, $n \geq 3$) are observed (Erickson et al., 2014; Gueneron et al., 2015). Recently, it was demonstrated that linear alkanes can be measured by PTR-MS with time-of-flight detector using NO^+ as reagent ions (NO^+ PTR-ToF-MS) (Inomata et al., 2014; Koss et al., 2016; Wang et al., 2020). These higher alkanes are ionized by NO^+ via hydride ion transfer leading to major product ions of $C_nH_{2n+1}^+$, with low degree of fragmentation (Inomata et al., 2014).

Meanwhile, it is interesting that cycloalkanes were also tried to be quantified using $C_nH_{2n+1}^+$ ions in H_3O^+ PTR-MS in oil and gas regions (Koss et al., 2017; Warneke et al., 2014; Yuan et al., 2014), though sensitivities were substantially low (~10% of other species) (Warneke et al., 2014). These evidences suggest that NO^+ ionization scheme could provide a possibility for measuring cycloalkanes along with acyclic alkanes, as demonstrated in ~~a two~~ recent ~~laboratory-chamber~~ work (Koss et al., 2016; Wang et al., 2022a).

In this study, we discuss the potential of online measurements of cycloalkanes in ambient air and ~~form~~ emission sources utilizing NO^+ ionization in PTR-ToF-MS. The results of laboratory experiments ~~of to characterization~~ characterize ~~of~~ product ions, calibration, and response time will be shown. Finally, measurements of cycloalkanes using NO^+ PTR-ToF-MS will be demonstrated from deployments at an urban site in southern China and a chassis dynamometer study for vehicular emissions.

2 Methods

2.1 NO^+ PTR-ToF-MS measurements

A commercially PTR-ToF-MS instrument (Ionicon Analytik, Austria) equipped with a quadrupole ion (Qi) guide for effective transfer of ions from drift tube to the time-of-flight mass spectrometer is used for this work (Sulzer et al., 2014), and the mass ~~resolving-resolution~~ approximately reach about 3000 m/ Δ m (Fig. S1). In order to generate NO^+ ions, 5 sccm ultra-high-purity air ($O_2+N_2 \geq 99.999\%$) is directed into to the hollow cathode discharge area of ion source, NO^+ ions are produced by ionization as follows (Federer et al., 1985; Karl et al., 2012):



For the purpose of ionize NO^+ ions to the greatest extent, reduce the generation of

impurity ions such as H_3O^+ , O_2^+ and NO_2^+ , the ion source voltage U_s and U_{so} were set to 40 V and 100 V, while drift tube voltages U_{dx} and U_{drift} were set to 23.5 V and 470 V with drift tube pressure at 3.8 mbar, resulting in an E/N (electric potential intensity relative to gas number density) of 60 Td. The specific details have been described in (Wang et al., 2020). The intensities of primary ions NO^+ and impurities including O_2^+ , NO_2^+ , and H_3O^+ and the ratio of O_2^+ to NO^+ during the measurements of urban air and vehicular emissions are shown in Fig. S2. The abundances of O_2^+ , NO_2^+ , and H_3O^+ are significantly lower than NO^+ ions and the ratio of O_2^+ to NO^+ is basically below 5% during the measurements of urban air expect for the period from 26 October to 2 November, 2018 (7-10%), while the ratio of O_2^+/NO^+ is basically below 2% during the measurements of vehicular emissions. (Wang et al., 2020). The measured ToF data is processed for high-resolution peak fitting using Tofware (Tofwerk AG, version, 3.0.3), obtaining high precision signals for cycloalkanes (Fig. S2S3). The signal of cycloalkanes used for quantification has been subtracted from the contribution of isotopes from other ions and other species such as unsaturated aldehydes that share the identical formula at the unit mass resolution (UMR) with cycloalkanes during the high-resolution peak fitting process. A description of the fitting and calculation methods are fully discussed in previous studies (Stark et al., 2015; Timonen et al., 2016). The raw ion count signals of NO^+ PTR-ToF-MS are normalized to the primary ion (NO^+) at a level of 10^6 cps to account for fluctuations of ion source and detector (see SI).

Compared to proton transfer reactions occurring mostly between H_3O^+ ions and VOCs species, NO^+ ions show a variety of reaction pathways with VOCs, which can be roughly summarized as follow:

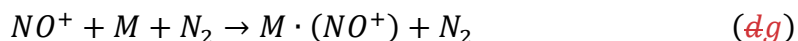
charge transfer:



hydride ion transfer:



association reaction:



As shown in Fig. 1, the ionization energy (IE) of VOC species is a determination factor for the reaction pathways with NO^+ . For example, as the IE of NO is 9.26 eV (Reiser et al., 1988), species with IE less than 9.26 eV, e.g., benzene and isoprene, will undergo charge transfer reaction (~~be~~) with NO^+ (Španěl and Smith, 1999, 1996), while species with IE greater than 9.26 eV, e.g., acetone and *n*-undecane, will undergo hydride ion transfer (~~ef~~) or association reaction (~~dg~~) with NO^+ (Amador-Muñoz et al., 2016; Diskin et al., 2002; Koss et al., 2016).

2.2 Calibration and correction experiments

In this study, we investigate characteristic ions of cycloalkanes ~~produced-undergo~~ ~~the generated by~~ NO^+ ionization from a series of species identification experiments. The information of cycloalkanes ~~chemicals-species~~ used in these experiments is listed in Table 1. In addition, we also evaluated potential interferences from mono-alkenes, the isomers of cycloalkanes. Calibration experiments were carried out to obtain sensitivities of cycloalkanes in both the laboratory and the field, using a customized cylinder gas standard (Apel-Riemer Environmental, Inc. USA), containing five different alkyl-cyclohexanes (C_{10} - C_{14}) and eight *n*-alkanes (C_8 - C_{15}) (Table S1).

Furthermore, some additional experiments were performed to explore the influences of humidity and tubing delay effects on measurements of cycloalkanes. Previously, it was shown that response factors of higher alkanes in NO^+ PTR-ToF-MS are slightly affected by air humidity, and the degree of influence is related to carbon number (Wang et al., 2020). Therefore, we evaluate the influence of humidity on ~~sensitivity-sensitivities~~ of cycloalkanes in NO^+ PTR-ToF-MS using a custom-built humidity delivery system (Fig. ~~S3S4~~), and the results are applied to explore the relationship between sensitivities of cycloalkanes and humidity. The perfluoroalkoxy (PFA) Teflon tubing is used for inlets in this study, but gas-wall partitioning can be important for low volatility compounds (Pagonis et al., 2017). As the result, measurements from controlled laboratory experiments and field deployments were

analyzed to systematically quantify and characterize tubing delay time of cycloalkanes.

3 Results and discussion

3.1 Characterization of product ion distribution

NO^+ PTR-ToF-MS was used to directly measure high-purity cycloalkane ~~chemicals-species~~ and identify the characteristic product ions produced by cycloalkanes under NO^+ ionization. Here, the major product ions, fragments and their contributions for different cycloalkanes are shown in Table 1. Chemical formulas of the product ions are determined based on the positions of measured mass peaks.

Fig. 2 shows mass spectra within the relevant range (m/z 60⁺ to 200⁺ Th) for cycloalkanes. The signals are normalized to the largest ion peak for better comparison. As shown in Fig. 2, no significant fragmentation appears for cycloheptane and methylcyclohexane (C_7H_{14}), and the dominating product ions are observed at m/z 97 Th, corresponding to $\text{C}_7\text{H}_{13}^+$. Similarly, the product ions generated by hexylcyclohexane and cyclododecane ($\text{C}_{12}\text{H}_{24}$) under NO^+ ionization mainly appear at m/z 167 Th (Fig. 2c-d), corresponding to $\text{C}_{12}\text{H}_{23}^+$, and fragments occurred at m/z 97 Th and m/z 111 Th, corresponding to $\text{C}_7\text{H}_{13}^+$ and $\text{C}_8\text{H}_{15}^+$, respectively. The product ions generated by cyclopentadecane and nonylcyclohexane ($\text{C}_{15}\text{H}_{30}$) mainly appear at m/z 209 Th, corresponding to $\text{C}_{15}\text{H}_{29}^+$, with slightly more fragmentation than C_{12} cyclic alkanes (Fig. S5). Bicyclic cycloalkanes undergo the same ionization channel from NO^+ ionization, as demonstrated by major product ions at m/z 165 Th ($\text{C}_{12}\text{H}_{21}^+$) and other fragmentation ions from bicyclohexyl ($\text{C}_{12}\text{H}_{22}$) (Fig. 2e). For instance, the mass spectra for C_{10} - C_{14} alkyl-cyclohexanes during the calibration experiments are shown in Fig.S6, with the same $\text{C}_n\text{H}_{2n-1}^+$ as the major product ions. ~~These results verify that reactions of cyclic and bicyclic alkanes with NO^+ ions follow the hydride ion transfer pathway to yield $\text{C}_n\text{H}_{2n-1}^+$ and $\text{C}_n\text{H}_{2n-3}^+$ product ions, respectively.~~ The fractions of M-H ions generated by high-purity cycloalkanes species including C_7 , C_{12} , and C_{15} cyclic alkanes and C_{12} bicyclic alkanes are summarized in Fig. S7. We observe that M-H ions account

for ~100% of total ion signals for C₇ cyclic alkanes and lower but comparable fractions (74-82%) for C₁₂ and C₁₅ cyclic alkanes.— These results verify that reactions of cyclic and bicyclic alkanes with NO⁺ ions follow the hydride ion transfer pathway to yield C_nH_{2n-1}⁺ and C_nH_{2n-3}⁺ product ions, respectively. As mentioned above, the characteristic peaks of cycloalkanes under NO⁺ ionization ~~is~~ are consistent with the ions that are received at the ~~for~~ attempts to utilize H₃O⁺ PTR-MS. ~~for~~ For the latter method though sensitivities are reported to be lower ~~cycloalkanes detection in previous studies, though with low sensitivities reported for cycloalkanes~~ (Erickson et al., 2014; Gueneron et al., 2015; Warneke et al., 2014; Yuan et al., 2014). As the result, we speculate that reactions of NO⁺ with cycloalkanes may present large contributions to cycloalkane M-H product ions in the H₃O⁺ chemistry mode of PTR-MS (Španěl et al., 1995).

~~As t~~ The isomers of cyclic alkanes, alkenes may interfere with measurements of cycloalkanes. Here, we use 1-heptene (C₇H₁₄) and 1-decene (C₁₀H₂₀), isomers of C₇ and C₁₀ cyclic alkanes, to explore the ionization regime of alkenes in NO⁺ chemical ionization (Fig. 3 and Table 1). These two alkenes produce more fragments than cycloalkanes under NO⁺ chemistry, but mainly react with NO⁺ via association reaction to yield C_nH_{2n}•(NO)⁺ product ions. The major product ions of 1-heptene and 1-decene appear at *m/z* 128 Th and *m/z* 170 Th, corresponding to C₇H₁₃HNO⁺ and C₁₀H₁₉HNO⁺, respectively. Based on the mass spectra, alkenes produce the C_nH_{2n-1}⁺ product ions at fractions of <5%, which are similar fragmentation ions from ~~to~~ NO⁺ ionization ~~results~~ of the two species and other 1-alkenes determined from a selected ion flow tube mass spectrometer (SIFT-MS) (Diskin et al., 2002). The same study (Diskin et al., 2002) also demonstrated that trans-2-alkenes might produce more C_nH_{2n-1}⁺ ions under NO⁺ ionization (e.g., trans-2-heptene contributions 40% of C₇H₁₃⁺ ions). However, concentrations of 1-alkenes and trans-2-alkenes in the atmosphere are usually significantly lower than cycloalkanes (about 25% and ~~<5%~~ 15%, respectively) (de Gouw et al., 2017; Yuan et al., 2013). We further compare the signals of C_nH_{2n}⁺ and C_nH_{2n-1}⁺ from calibration experiments, urban air measurements and chassis

dynamometer study (Fig. S8). The typical ratios of $C_nH_{2n}^+/C_nH_{2n-1}^+$ for cyclic alkanes are in the range of 2-6%, with similar ratios determined from urban air measurements (3-7%). The ratios of $C_nH_{2n}^+$ to $C_nH_{2n-1}^+$ from vehicular emissions maintained at 6-16% for C_{10} - C_{14} ions, which is a little bit higher than those determined from cyclic alkanes, while the ratios of C_{15} - C_{20} ions are comparable with pure cyclic alkanes (4-8%). Even though all of these differences are attributed to potential interference from 2-alkenes and assume the same quantity of $C_nH_{2n-1}^+$ and $C_nH_{2n}^+$ ions from NO^+ ionization from 2-alkenes, the upper limits of the interference from alkenes should be in the range of 1-2% for urban air measurements and 2-12% for measurements of vehicular emissions. Therefore, we conclude that the interferences ~~of~~ from alkenes to cyclic alkanes ~~on~~ measurements of cycloalkanes in most environments are ~~small~~ minor.

3.2 Sensitivity, humidity dependence and detection limits

The calibration experiments of cycloalkanes (see details of gas standard in Table S1) are carried out in both dry conditions (<1% RH) and humidified conditions (Fig. S5S9). Fig. 4 illustrates results from a typical calibration experiment for five different alkyl-substituted cyclohexanes with carbon atoms of 10-14 in dry air (relative humidity < 1%) for NO^+ PTR-ToF-MS. There is a good linear relationship between ion signals and concentrations of various cycloalkanes ($R=0.9996$ - 0.9999). Sensitivities (ncps ppb⁻¹) of cycloalkanes are in the range of 210 to 260 ncps ppb⁻¹ (Table 2). The sensitivity of each cycloalkanes remained stable in the long-term calibration conducted in the laboratory and in the field (Fig. S6S10). Table 2 further shows detection limits of cycloalkanes by NO^+ PTR-ToF-MS, which are calculated as the concentrations with the signal-to-noise ratio of 3 (Bertram et al., 2011; Yuan et al., 2017). The detection limits of cycloalkanes at integral time of 10 s and 1 min are in the range of 6.2 to 8.2 ppt and 2.4-3.6 ppt, respectively. For comparison, the detection limits of NO^+ PTR-ToF-MS for 24 h of integral time are also determined, obtaining comparable results (<0.1 ppt) with detection limits of GC×GC-ToF-MS (0.1-0.3 ppt for daily sample) (Liang et al., 2018; Xu et al., 2020a),.

Fig. 4b shows that normalized signals of hexylcyclohexane relative to dry conditions as a function of different humidity. The relative signals of the explored cycloalkanes show minor decrease (<10%) at the highest humidity (~82% RH at 25°C) compare to dry condition, and the observed changes for cycloalkanes with different carbon number are similar, suggesting little influence of humidity on measurements of cycloalkanes. The humidity-dependence curves determined in Fig. 4b are used to corrected variations of ambient humidity in the atmosphere.

The response time of various cycloalkanes in the instrument and also sampling tubing is determined from laboratory experiments (Fig. S6S11). For the species not in the gas standard, we also take advantage of vehicular emissions measurements associated with high concentrations of cycloalkanes, and the sampling methods are same as mentioned in Li et al. (2021b) and Wang et al. (2022b). Here, we use the delay time to determine response of cycloalkanes, which is calculated based on the time it takes for signals to drop to 10% of its initial value (Fig. S7S12) (Pagonis et al., 2017). The delay time of cycloalkanes are summarized in Fig. 5. The delay time of various cycloalkanes generally increases with the carbon numbers, ranging from a few seconds to a few minutes, but relatively lower than determined for those acyclic alkanes within C₁₀-C₁₅ range (Wang et al., 2020). These results suggest that measured variability of cycloalkanes with higher carbon number, especially for C₁₉-C₂₀ or above, may only be reliable for time scales longer than 10 min.

3.3 Applications in ambient air and vehicular exhausts

Based on the results shown above, we deployed the NO⁺ PTR-ToF-MS to measure concentration levels and variations of cycloalkanes at an urban site in Guangzhou, southern China. Details of the field campaign were described in previous studies (Wang et al., 2020; Wu et al., 2020). The average sensitivities of long-term calibration (dry condition) during the field observations were used to quantify cycloalkanes after corrected variations of ambient humidity in the atmosphere. For the cycloalkanes that are not contained in the gas standard, we employ average sensitivity for calibrated

cycloalkanes in gas standard.

The concentration levels and diurnal profiles of cyclic and bicyclic alkanes are illustrated in Fig. 6a, along with CO. In general, cyclic and bicyclic alkanes demonstrated similar temporal variability as CO, suggesting cyclic and bicyclic alkanes may be mainly emitted from primary combustion sources. Concentrations of C₁₂ bicyclic alkanes are observed to be comparable with C₁₂ cyclic alkanes. As shown in Fig. 6b, selected C₁₀ and C₁₂ cycloalkanes show diurnal variations with lower concentration during the daytime. Compared to diurnal variations of other species with different reactivity (Wu et al., 2020), the decline fractions of cycloalkanes are more comparable to reactive species (e.g., C₈ aromatics) than the inert ones (e.g., CO, benzene), indicating significantly daytime photochemical removal of these cycloalkanes. Diurnal patterns of other cyclic and bicyclic alkanes exhibit similar results (Fig. S8S13). As discussed in Wang et al. (2020), similar diurnal profiles of cycloalkanes with different carbon number also imply that tubing-delay effect may not affect significantly to temporal variations of cycloalkanes reported here. Based on both time series and correlation analysis (Fig. 6c), cyclic and bicyclic alkanes showed strong correlation with acyclic alkanes, ~~suggesting they came from same emission sources~~suggesting they predominantly came from same emission sources.

NO⁺ PTR-ToF-MS was also applied to measure cycloalkanes emissions along with other organic compounds from vehicles using gasoline, diesel, and LPG as fuel, by conducting a chassis dynamometer measurement (Wang et al., 2022b). Fig. 7 shows time series of C₁₂ cyclic and bicyclic alkanes, C₁₂ alkanes, toluene, and acetaldehyde measured by NO⁺ PTR-ToF-MS for a gasoline vehicle with emission standard of China III and a diesel vehicle with emission standard of China IV. Both test vehicles were started with hot engines. As shown in Fig. 7a, high concentrations of selected cycloalkanes emitted by the gasoline vehicle were observed as the engine started. Compared with typical VOC compounds exhausted by vehicles (e.g., toluene and acetaldehyde), concentrations of cycloalkanes were lower but showed similar temporal

variations. In comparison, cycloalkanes emissions from diesel vehicles are obviously different. As shown in Fig. 7b, concentrations of cycloalkanes showed relatively moderate enhancements as engine started, but significantly enhanced with high vehicle speed, obtaining periodic pattern variations within each test cycle. Though the highest concentrations of cycloalkanes observed for gasoline and diesel vehicles are similar, determined emission factors of diesel vehicles are significantly larger than gasoline vehicles, since emissions of cycloalkanes are mainly concentrated during a short period at engine start for gasoline vehicles, whereas emissions of cycloalkanes remain high during hot running for diesel vehicles. For instance, the determined emission factors of C₁₂ cyclic alkanes are 0.06 mg km⁻¹ for gasoline vehicle and 1.17 mg km⁻¹ for diesel vehicles, respectively. In addition to cycloalkanes and alkanes, other compounds including aromatics and oxygenated VOCs also demonstrate larger differences between gasoline and diesel vehicles, which were mainly attributed to different chemical compositions of gasoline and diesel fuels (Wang et al., 2022b). ~~(Huang et al., 2022; Qi et al., 2021; Sun et al., 2021)~~ Recent studies reported that cyclic compounds occupied a large proportion in IVOCs emitted from vehicles, with prominent SOA formation potentials (Fang et al., 2021; Huang et al., 2018; Zhao et al., 2016), but emissions of individual cycloalkanes were not reported yet. As the result, high time-resolution measurements of cycloalkanes from vehicular emissions by NO⁺ PTR-ToF-MS can improve the characterization of emission mechanisms of these species.

3.4 Insights from simultaneous measurements of cycloalkanes and alkanes

Since NO⁺ PTR-ToF-MS can provide simultaneous measurements of cycloalkanes and acyclic alkanes, we can use this information to explore the relative importance of cycloalkanes. Fig. 8 shows mean concentrations of cycloalkanes (cyclic and bicyclic) and alkanes with different carbon numbers (C₁₀-C₂₀) measured by NO⁺ PTR-ToF-MS in urban air and emissions from diesel vehicles. In urban region, concentrations of cyclic and bicyclic cycloalkanes are comparable, but lower than acyclic alkanes, with

concentration ratios relative to acyclic alkanes in the range of 0.30-0.46 for cyclic alkanes and 0.23-0.51 for bicyclic alkanes. Similar results are obtained for gasoline vehicles, with cyclic alkanes/acyclic alkanes and bicyclic alkanes/acyclic ratios of 0.27-0.53 for and 0.21-0.52, respectively (Fig. 98). The contributions of cycloalkanes in diesel vehicular emissions are relatively higher, with the concentration ratios relative to acyclic alkanes in the range of 0.42-0.66 for cyclic alkanes and 0.37-0.95 for bicyclic alkanes.

As there ~~is~~ are only limited measurements of bicyclic alkanes in the literature, we compare concentration ratios of cyclic alkanes to acyclic alkanes with results in previous studies, mainly ~~determined from measurements using gas chromatography techniques by~~ (GC-MS/FID and GC×GC). The details of the technique used in these earlier studies are summarized in Table S2. As shown in the Fig. 9, the ratios obtained in the urban region of Guangzhou in this work (0.2-0.4) are similar to other measurements in urban area, including ~~London, UK (Xu et al., 2020b) and~~ Algiers, Algeria (Yassaa et al., 2001). ~~(Xu et al., 2020b).~~ The ratios obtained in London, UK (Xu et al., 2020b) are higher than the ratios obtained in Guangzhou, but similar to the diesel exhaust in our work for C₁₃-C₁₈ range. These results are likely due to the measurement location in London is proximity to a main road, cyclic and acyclic alkanes may be dominated by traffic emissions with high fractions of diesel vehicles in fleet. Although some variations observed in different urban environments, nevertheless, these ratios are broadly within the range between gasoline and diesel emissions. As for emissions from diesel vehicles, the ratios measured in this study are similar to GC×GC measurements in UK (Alam et al., 2016) for C₁₂-C₁₄ range and GC-MS measurements in USA (Gentner et al., 2012), whereas the ratios from this study are higher than Alam et al. (2016) for larger carbon number. The relative fractions of cycloalkanes measured from oil and gas region (Gilman et al., 2013) and emissions from lubricating oil (Liang et al., 2018) (>0.7) are relatively higher than ambient air and vehicular emissions. The variability pattern of cyclic alkanes to acyclic alkanes ratios for different carbon number

may be used for source analysis of these IVOCs in the future.

4 Conclusion

In this study, we show that online measurements of cycloalkanes can be achieved using proton transfer reaction time-of-flight mass spectrometry with NO^+ chemical ionization (NO^+ PTR-ToF-MS). Our results demonstrate that cyclic and bicyclic alkanes are ionized via hydride ion transfer leading to characteristic product ions of $\text{C}_n\text{H}_{2n-1}^+$ and $\text{C}_n\text{H}_{2n-3}^+$, respectively. As isomers of cycloalkanes, alkenes undergoes association reactions mainly yielding product ions $\text{C}_n\text{H}_{2n}\bullet(\text{NO})^+$, which induce little interference to cycloalkanes detection. Calibration of various cycloalkanes show similar sensitivities with small humidity dependence. The detection limits of cycloalkanes are in the range of 2-4 ppt at integral time of 1 min.

Applying this method, cycloalkanes were successfully measured at an urban site in southern China and a chassis dynamometer study for vehicular emissions. Concentrations of both cyclic and bicyclic alkanes are substantial in urban air and vehicular emissions. Diurnal variations of cycloalkanes in the urban air indicate significant losses due to photochemical processes during the daytime. The concentration ratios of cyclic alkanes to acyclic alkanes are similar between urban air and gasoline vehicle emissions, but higher for diesel vehicles, which could be potentially used for source analysis in future studies. Our work demonstrates that NO^+ PTR-ToF-MS provides a new complementary approach for fast characterization of cycloalkanes in both ambient air and emission sources, which can be helpful to investigate sources of cycloalkanes and their contribution to SOA formation in the atmosphere. Measurements of cycloalkanes in the particle phase may also be possible by combining NO^+ PTR-ToF-MS with “chemical analysis of aerosols online” (CHARON) or other similar aerosol inlets (Muller et al., 2017), which could further provide particle-phase information of cycloalkanes and gas-partitioning analysis of cycloalkanes.

Data availability

Data are available from the authors upon request.

Author contribution

BY designed the research. YBC, CMW, SHW, XJH, CHW, XS, YBH, XBL, YJL and MS contributed to data collection. YBC performed data analysis, with contributions from CMW, SHW, XJH, and CHW. YBC and BY prepared the manuscript with contributions from other authors. All the authors reviewed the manuscript.

Competing interests

The authors declare that they have no known competing financial interests or personal relationships that could have appeared to influence the work reported in this paper.

Acknowledgement

This work was supported by the National Natural Science Foundation of China (grant No. 41877302, 42121004), Key-Area Research and Development Program of Guangdong Province (grant No. 2020B1111360003), and Guangdong Innovative and Entrepreneurial Research Team Program (grant No. 2016ZT06N263). This work was also supported by Special Fund Project for Science and Technology Innovation Strategy of Guangdong Province (Grant No.2019B121205004).

Reference

Aklilu, Y.-a., Cho, S., Zhang, Q., and Taylor, E.: Source apportionment of volatile organic compounds measured near a cold heavy oil production area, *Atmospheric Research*, 206, 75-86, 2018.

Alam, M. S., Zeraati-Rezaei, S., Liang, Z., Stark, C., Xu, H., Mackenzie, A. R., and Harrison, R. M.: Mapping and quantifying isomer sets of hydrocarbons ($\geq C_{12}$) in diesel exhaust, lubricating oil and diesel fuel samples using GC \times GC-ToF-MS, *Atmospheric Measurement Techniques*, 11, 3047-3058, 2018.

-
- Alam, M. S., Zeraati-Rezaei, S., Stark, C. P., Liang, Z., Xu, H., and Harrison, R. M.: The characterisation of diesel exhaust particles – composition, size distribution and partitioning, *Faraday Discussions*, 189, 69-84, 2016.
- Amador-Muñoz, O., Misztal, P. K., Weber, R., Worton, D. R., Zhang, H., Drozd, G., and Goldstein, A. H.: Sensitive detection of *n*-alkanes using a mixed ionization mode proton-transfer-reaction mass spectrometer, *Atmospheric Measurement Techniques*, 9, 5315-5329, 2016.
- Bertram, T. H., Kimmel, J. R., Crisp, T. A., Ryder, O. S., Yatavelli, R. L. N., Thornton, J. A., Cubison, M. J., Gonin, M., and Worsnop, D. R.: A field-deployable, chemical ionization time-of-flight mass spectrometer, *Atmospheric Measurement Techniques*, 4, 1471-1479, 2011.
- de Gouw, J. and Warneke, C.: Measurements of volatile organic compounds in the earth's atmosphere using proton-transfer-reaction mass spectrometry, *Mass Spectrom Rev*, 26, 223-257, 2007.
- de Gouw, J. A.: Budget of organic carbon in a polluted atmosphere: Results from the New England Air Quality Study in 2002, *Journal of Geophysical Research*, 110, 2005.
- de Gouw, J. A., Gilman, J. B., Kim, S. W., Lerner, B. M., Isaacman-VanWertz, G., McDonald, B. C., Warneke, C., Kuster, W. C., Lefer, B. L., Griffith, S. M., Dusanter, S., Stevens, P. S., and Stutz, J.: Chemistry of Volatile Organic Compounds in the Los Angeles basin: Nighttime Removal of Alkenes and Determination of Emission Ratios, *Journal of Geophysical Research: Atmospheres*, 122, 11,843-811,861, 2017.
- Diskin, A. M., Wang, T. S., Smith, D., and Spanel, P.: A selected ion flow tube (SIFT), study of the reactions of H_3O^+ , NO^+ and O_2^+ ions with a series of alkenes; in support of SIFT-MS, *International Journal of Mass Spectrometry*, 218, 87-101, 2002.
- Donahue, N. M., Kroll, J. H., Pandis, S. N., and Robinson, A. L.: A two-dimensional volatility basis set - Part 2: Diagnostics of organic-aerosol evolution, *Atmospheric Chemistry and Physics*, 12, 615-634, 2012.

Erickson, M. H., Gueneron, M., and Jobson, B. T.: Measuring long chain alkanes in diesel engine exhaust by thermal desorption PTR-MS, *Atmospheric Measurement Techniques*, 7, 225-239, 2014.

Fang, H., Huang, X., Zhang, Y., Pei, C., Huang, Z., Wang, Y., Chen, Y., Yan, J., Zeng, J., Xiao, S., Luo, S., Li, S., Wang, J., Zhu, M., Fu, X., Wu, Z., Zhang, R., Song, W., Zhang, G., Hu, W., Tang, M., Ding, X., Bi, X., and Wang, X.: Measurement report: Emissions of intermediate-volatility organic compounds from vehicles under real-world driving conditions in an urban tunnel, *Atmospheric Chemistry and Physics*, 21, 10005-10013, 2021.

Federer, W., Dobler, W., Howorka, F., Lindinger, W., Durup - Ferguson, M., and Ferguson, E. E.: Collisional relaxation of vibrationally excited $\text{NO}^+(\text{v})$ ions, *The Journal of Chemical Physics*, 83, 1032-1038, 1985.

Gentner, D. R., Isaacman, G., Worton, D. R., Chan, A. W., Dallmann, T. R., Davis, L., Liu, S., Day, D. A., Russell, L. M., Wilson, K. R., Weber, R., Guha, A., Harley, R. A., and Goldstein, A. H.: Elucidating secondary organic aerosol from diesel and gasoline vehicles through detailed characterization of organic carbon emissions, *Proceedings of the National Academy of Sciences of the United States of America*, 109, 18318-18323, 2012.

Gilman, J. B., Lerner, B. M., Kuster, W. C., and de Gouw, J. A.: Source Signature of Volatile Organic Compounds from Oil and Natural Gas Operations in Northeastern Colorado, *Environmental Science & Technology*, 47, 1297-1305, 2013.

Goldstein, A. H. and Galbally, I. E.: Known and unknown organic constituents in the Earth's atmosphere, *Environmental Science & Technology*, 41, 1514-1521, 2007.

Gueneron, M., Erickson, M. H., VanderSchelden, G. S., and Jobson, B. T.: PTR-MS fragmentation patterns of gasoline hydrocarbons, *International Journal of Mass Spectrometry*, 379, 97-109, 2015.

He, X., Yuan, B., Wu, C., Wang, S., Wang, C., Huangfu, Y., Qi, J., Ma, N., Xu, W., Wang, M., Chen, W., Su, H., Cheng, Y., and Shao, M.: Volatile organic compounds in

wintertime North China Plain: Insights from measurements of proton transfer reaction time-of-flight mass spectrometer (PTR-ToF-MS), *Journal of Environmental Sciences*, 114, 98-114, 2022.

Hu, W., Zhou, H., Chen, W., Ye, Y., Pan, T., Wang, Y., Song, W., Zhang, H., Deng, W., Zhu, M., Wang, C., Wu, C., Ye, C., Wang, Z., Yuan, B., Huang, S., Shao, M., Peng, Z., Day, D. A., Campuzano-Jost, P., Lambe, A. T., Worsnop, D. R., Jimenez, J. L., and Wang, X.: Oxidation Flow Reactor Results in a Chinese Megacity Emphasize the Important Contribution of S/IVOCs to Ambient SOA Formation, *Environmental Science & Technology*, 56, 6880-6893, 2022.

Huang, C., Hu, Q., Li, Y., Tian, J., Ma, Y., Zhao, Y., Feng, J., An, J., Qiao, L., Wang, H., Jing, S. A., Huang, D., Lou, S., Zhou, M., Zhu, S., Tao, S., and Li, L.: Intermediate Volatility Organic Compound Emissions from a Large Cargo Vessel Operated under Real-World Conditions, *Environmental Science & Technology*, 52, 12934-12942, 2018.

Huang, J., Yuan, Z., Duan, Y., Liu, D., Fu, Q., Liang, G., Li, F., and Huang, X.: Quantification of temperature dependence of vehicle evaporative volatile organic compound emissions from different fuel types in China, *Sci Total Environ*, 813, 152661, 2022.

Hunter, J. F., Carrasquillo, A. J., Daumit, K. E., and Kroll, J. H.: Secondary organic aerosol formation from acyclic, monocyclic, and polycyclic alkanes, *Environmental Science & Technology*, 48, 10227-10234, 2014.

Inomata, S., Tanimoto, H., and Yamada, H.: Mass Spectrometric Detection of Alkanes Using NO⁺ Chemical Ionization in Proton-transfer-reaction Plus Switchable Reagent Ion Mass Spectrometry, *Chemistry Letters*, 43, 538-540, 2014.

Jahn, L. G., Wang, D. S., Dhulipala, S. V., and Ruiz, L. H.: Gas-Phase Chlorine Radical Oxidation of Alkanes: Effects of Structural Branching, NO_x, and Relative Humidity Observed during Environmental Chamber Experiments, *The Journal of Physical Chemistry A*, 125, 7303-7317, 2021.

Karl, T., Hansel, A., Cappellin, L., Kaser, L., Herdinger-Blatt, I., and Jud, W.:

Selective measurements of isoprene and 2-methyl-3-buten-2-ol based on NO^+ ionization mass spectrometry, *Atmospheric Chemistry and Physics*, 12, 11877-11884, 2012.

Koss, A., Yuan, B., Warneke, C., Gilman, J. B., Lerner, B. M., Veres, P. R., Peischl, J., Eilerman, S., Wild, R., Brown, S. S., Thompson, C. R., Ryerson, T., Hanisco, T., Wolfe, G. M., Clair, J. M. S., Thayer, M., Keutsch, F. N., Murphy, S., and de Gouw, J.: Observations of VOC emissions and photochemical products over US oil- and gas-producing regions using high-resolution H_3O^+ CIMS (PTR-ToF-MS), *Atmospheric Measurement Techniques*, 10, 2941-2968, 2017.

Koss, A. R., Warneke, C., Yuan, B., Coggon, M. M., Veres, P. R., and de Gouw, J. A.: Evaluation of NO^+ reagent ion chemistry for online measurements of atmospheric volatile organic compounds, *Atmospheric Measurement Techniques*, 9, 2909-2925, 2016.

Li, J., Wang, W., Li, K., Zhang, W., Peng, C., Liu, M., Chen, Y., Zhou, L., Li, H., and Ge, M.: Effect of chemical structure on optical properties of secondary organic aerosols derived from C_{12} alkanes, *Science of The Total Environment*, 751, 141620, 2021a.

Li, T., Wang, Z., Yuan, B., Ye, C., Lin, Y., Wang, S., Sha, Q. e., Yuan, Z., Zheng, J., and Shao, M.: Emissions of carboxylic acids, hydrogen cyanide (HCN) and isocyanic acid (HNCO) from vehicle exhaust, *Atmospheric Environment*, 247, 2021b.

Li, Y., Ren, B., Qiao, Z., Zhu, J., Wang, H., Zhou, M., Qiao, L., Lou, S., Jing, S., Huang, C., Tao, S., Rao, P., and Li, J.: Characteristics of atmospheric intermediate volatility organic compounds (IVOCs) in winter and summer under different air pollution levels, *Atmospheric Environment*, 210, 58-65, 2019.

Liang, Z., Chen, L., Alam, M. S., Zeraati Rezaei, S., Stark, C., Xu, H., and Harrison, R. M.: Comprehensive chemical characterization of lubricating oils used in modern vehicular engines utilizing $\text{GC} \times \text{GC}$ -TOFMS, *Fuel*, 220, 792-799, 2018.

Lim, Y. B. and Ziemann, P. J.: Effects of Molecular Structure on Aerosol Yields

from OH Radical-Initiated Reactions of Linear, Branched, and Cyclic Alkanes in the Presence of NO_x, *Environmental Science & Technology*, 43, 2328-2334, 2009.

Lou, H., Hao, Y., Zhang, W., Su, P., Zhang, F., Chen, Y., Feng, D., and Li, Y.: Emission of intermediate volatility organic compounds from a ship main engine burning heavy fuel oil, *Journal of Environmental Sciences*, 84, 197-204, 2019.

Loza, C. L., Craven, J. S., Yee, L. D., Coggon, M. M., Schwantes, R. H., Shiraiwa, M., Zhang, X., Schilling, K. A., Ng, N. L., Canagaratna, M. R., Ziemann, P. J., Flagan, R. C., and Seinfeld, J. H.: Secondary organic aerosol yields of 12-carbon alkanes, *Atmospheric Chemistry and Physics*, 14, 1423-1439, 2014.

Monks, P. S., Archibald, A. T., Colette, A., Cooper, O., Coyle, M., Derwent, R., Fowler, D., Granier, C., Law, K. S., Mills, G. E., Stevenson, D. S., Tarasova, O., Thouret, V., von Schneidemesser, E., Sommariva, R., Wild, O., and Williams, M. L.: Tropospheric ozone and its precursors from the urban to the global scale from air quality to short-lived climate forcer, *Atmospheric Chemistry and Physics*, 15, 8889-8973, 2015.

Muller, M., Eichler, P., D'Anna, B., Tan, W., and Wisthaler, A.: Direct Sampling and Analysis of Atmospheric Particulate Organic Matter by Proton-Transfer-Reaction Mass Spectrometry, *Anal Chem*, 89, 10889-10897, 2017.

Pagonis, D., Krechmer, J. E., de Gouw, J., Jimenez, J. L., and Ziemann, P. J.: Effects of gas-wall partitioning in Teflon tubing and instrumentation on time-resolved measurements of gas-phase organic compounds, *Atmospheric Measurement Techniques*, 10, 4687-4696, 2017.

Qi, L., Zhao, J., Li, Q., Su, S., Lai, Y., Deng, F., Man, H., Wang, X., Shen, X., Lin, Y., Ding, Y., and Liu, H.: Primary organic gas emissions from gasoline vehicles in China: Factors, composition and trends, *Environ Pollut*, 290, 117984, 2021.

Reiser, G., Habenicht, W., Müller-Dethlefs, K., and Schlag, E. W.: The ionization energy of nitric oxide, *Chemical Physics Letters*, 152, 119-123, 1988.

Robinson, A. L., Donahue, N. M., Shrivastava, M. K., Weitkamp, E. A., Sage, A. M., Grieshop, A. P., Lane, T. E., Pierce, J. R., and Pandis, S. N.: Rethinking Organic

569 Aerosols: Semivolatile Emissions and Photochemical Aging, *Science*, 315, 1259-1262,
570 2007.

571 Španěl, P., Pavlik, M., and Smith, D.: Reactions of H_3O^+ and OH^- ions with some
572 organic molecules; applications to trace gas analysis in air, *International Journal of*
573 *Mass Spectrometry and Ion Processes*, 145, 177-186, 1995.

574 Španěl, P. and Smith, D.: Selected ion flow tube studies of the reactions of H_3O^+ ,
575 NO^+ , and O_2^+ with several aromatic and aliphatic monosubstituted halocarbons,
576 *International Journal of Mass Spectrometry*, 189, 213-223, 1999.

577 Španěl, P. and Smith, D.: A selected ion flow tube study of the reactions of NO^+ and
578 O_2^+ ions with some organic molecules: The potential for trace gas analysis of air, *The*
579 *Journal of Chemical Physics*, 104, 1893-1899, 1996.

580 Stark, H., Yatavelli, R. L. N., Thompson, S. L., Kimmel, J. R., Cubison, M. J.,
581 Chhabra, P. S., Canagaratna, M. R., Jayne, J. T., Worsnop, D. R., and Jimenez, J. L.:
582 Methods to extract molecular and bulk chemical information from series of complex
583 mass spectra with limited mass resolution, *International Journal of Mass Spectrometry*,
584 389, 26-38, 2015.

585 Sulzer, P., Hartungen, E., Hanel, G., Feil, S., Winkler, K., Mutschlechner, P.,
586 Haidacher, S., Schottkowsky, R., Gunsch, D., Seehauser, H., Striednig, M., Jürschik, S.,
587 Breiev, K., Lanza, M., Herbig, J., Märk, L., Märk, T. D., and Jordan, A.: A Proton
588 Transfer Reaction-Quadrupole interface Time-Of-Flight Mass Spectrometer (PTR-
589 QiTOF): High speed due to extreme sensitivity, *International Journal of Mass*
590 *Spectrometry*, 368, 1-5, 2014.

591 Sun, L., Zhong, C., Peng, J., Wang, T., Wu, L., Liu, Y., Sun, S., Li, Y., Chen, Q.,
592 Song, P., and Mao, H.: Refueling emission of volatile organic compounds from China
593 6 gasoline vehicles, *Sci Total Environ*, 789, 147883, 2021.

594 Timonen, H., Cubison, M., Aurela, M., Brus, D., Lihavainen, H., Hillamo, R.,
595 Canagaratna, M., Nekat, B., Weller, R., Worsnop, D., and Saarikoski, S.: Applications
596 and limitations of constrained high-resolution peak fitting on low resolving power mass

spectra from the ToF-ACSM, *Atmospheric Measurement Techniques*, 9, 3263-3281, 2016.

Tkacik, D. S., Presto, A. A., Donahue, N. M., and Robinson, A. L.: Secondary Organic Aerosol Formation from Intermediate-Volatility Organic Compounds: Cyclic, Linear, and Branched Alkanes, *Environmental Science & Technology*, 46, 8773-8781, 2012.

Wang, C. M., Yuan, B., Wu, C. H., Wang, S. H., Qi, J. P., Wang, B. L., Wang, Z. L., Hu, W. W., Chen, W., Ye, C. S., Wang, W. J., Sun, Y. L., Wang, C., Huang, S., Song, W., Wang, X. M., Yang, S. X., Zhang, S. Y., Xu, W. Y., Ma, N., Zhang, Z. Y., Jiang, B., Su, H., Cheng, Y. F., Wang, X. M., and Shao, M.: Measurements of higher alkanes using NO⁺ chemical ionization in PTR-ToF-MS: important contributions of higher alkanes to secondary organic aerosols in China, *Atmospheric Chemistry and Physics*, 20, 14123-14138, 2020.

Wang, K., Wang, W., Fan, C., Li, J., Lei, T., Zhang, W., Shi, B., Chen, Y., Liu, M., Lian, C., Wang, Z., and Ge, M.: Reactions of C12-C14 n-Alkylcyclohexanes with Cl Atoms: Kinetics and Secondary Organic Aerosol Formation, *Environmental Science & Technology*, 56, 4859-4870, 2022a.

Wang, S., Yuan, B., Wu, C., Wang, C., Li, T., He, X., Huangfu, Y., Qi, J., Li, X. B., Sha, Q., Zhu, M., Lou, S., Wang, H., Karl, T., Graus, M., Yuan, Z., and Shao, M.: Oxygenated volatile organic compounds (VOCs) as significant but varied contributors to VOC emissions from vehicles, *Atmospheric Chemistry and Physics*, 22, 9703-9720, 2022b.

Warneke, C., Geiger, F., Edwards, P. M., Dube, W., Pétron, G., Kofler, J., Zahn, A., Brown, S. S., Graus, M., Gilman, J. B., Lerner, B. M., Peischl, J., Ryerson, T. B., de Gouw, J. A., and Roberts, J. M.: Volatile organic compound emissions from the oil and natural gas industry in the Uintah Basin, Utah: oil and gas well pad emissions compared to ambient air composition, *Atmospheric Chemistry and Physics*, 14, 10977-10988, 2014.

Wu, C., Wang, C., Wang, S., Wang, W., Yuan, B., Qi, J., Wang, B., Wang, H., Wang, C., Song, W., Wang, X., Hu, W., Lou, S., Ye, C., Peng, Y., Wang, Z., Huangfu, Y., Xie, Y., Zhu, M., Zheng, J., Wang, X., Jiang, B., Zhang, Z., and Shao, M.: Measurement report: Important contributions of oxygenated compounds to emissions and chemistry of volatile organic compounds in urban air, *Atmospheric Chemistry and Physics*, 20, 14769-14785, 2020.

Xing, L. Q., Wang, L. C., and Zhang, R.: Characteristics and health risk assessment of volatile organic compounds emitted from interior materials in vehicles: a case study from Nanjing, China, *Environmental Science and Pollution Research*, 25, 14789-14798, 2018.

Xu, R., Alam, M. S., Stark, C., and Harrison, R. M.: Behaviour of traffic emitted semi-volatile and intermediate volatility organic compounds within the urban atmosphere, *Science of The Total Environment*, 720, 2020a.

Xu, R., Alam, M. S., Stark, C., and Harrison, R. M.: Composition and emission factors of traffic- emitted intermediate volatility and semi-volatile hydrocarbons (C₁₀–C₃₆) at a street canyon and urban background sites in central London, UK, *Atmospheric Environment*, 231, 2020b.

Yassaa, N., Meklati, B. Y., Brancaleoni, E., Frattoni, M., and Ciccioli, P.: Polar and non-polar volatile organic compounds (VOCs) in urban Algiers and saharian sites of Algeria, *Atmospheric Environment*, 35, 787-801, 2001.

Yee, L. D., Craven, J. S., Loza, C. L., Schilling, K. A., Ng, N. L., Canagaratna, M. R., Ziemann, P. J., Flagan, R. C., and Seinfeld, J. H.: Effect of chemical structure on secondary organic aerosol formation from C₁₂ alkanes, *Atmospheric Chemistry and Physics*, 13, 11121-11140, 2013.

Yuan, B., Hu, W. W., Shao, M., Wang, M., Chen, W. T., Lu, S. H., Zeng, L. M., and Hu, M.: VOC emissions, evolutions and contributions to SOA formation at a receptor site in eastern China, *Atmospheric Chemistry and Physics*, 13, 8815-8832, 2013.

653 Yuan, B., Koss, A. R., Warneke, C., Coggon, M., Sekimoto, K., and de Gouw, J.
654 A.: Proton-Transfer-Reaction Mass Spectrometry: Applications in Atmospheric
655 Sciences, *Chem Rev*, 117, 13187-13229, 2017.

656 Yuan, B., Warneke, C., Shao, M., and de Gouw, J. A.: Interpretation of volatile
657 organic compound measurements by proton-transfer-reaction mass spectrometry over
658 the deepwater horizon oil spill, *International Journal of Mass Spectrometry*, 358, 43-48,
659 2014.

660 Zhao, Y., Hennigan, C. J., May, A. A., Tkacik, D. S., De Gouw, J. A., Gilman, J.
661 B., Kuster, W. C., Borbon, A., and Robinson, A. L.: Intermediate-Volatility Organic
662 Compounds: A Large Source of Secondary Organic Aerosol, *Environmental Science &*
663 *Technology*, 48, 13743-13750, 2014.

664 Zhao, Y., Nguyen, N. T., Presto, A. A., Hennigan, C. J., May, A. A., and Robinson,
665 A. L.: Intermediate Volatility Organic Compound Emissions from On-Road Diesel
666 Vehicles: Chemical Composition, Emission Factors, and Estimated Secondary Organic
667 Aerosol Production, *Environmental Science & Technology*, 49, 11516-11526, 2015.

668 Zhao, Y., Nguyen, N. T., Presto, A. A., Hennigan, C. J., May, A. A., and Robinson,
669 A. L.: Intermediate Volatility Organic Compound Emissions from On-Road Gasoline
670 Vehicles and Small Off-Road Gasoline Engines, *Environmental Science & Technology*,
671 50, 4554-4563, 2016.

672

Table 1. The formula, purity, ionization energy (IE) of the ~~chemicals-species~~ used in product ion characterization experiments are shown. The percentage of each product ion from the reactions with NO⁺ ions is indicated in brackets, and the major product ions are identified in bold.

Chemicals <u>Species</u>	Formula	Purity (%)	IE ^a (eV)	Product ions (%)		
Cycloheptane	C ₇ H ₁₄	98.0%	9.82	C₇H₁₃⁺(100)		
Methylcyclohexane	C ₇ H ₁₄	99.0%	9.64	C₇H₁₃⁺(100)		
Cyclododecane	C ₁₂ H ₂₄	99.0%	9.72	C₁₂H₂₃⁺(82)	C ₈ H ₁₅ ⁺ (8)	C ₇ H ₁₃ ⁺ (10)
Hexylcyclohexane	C ₁₂ H ₂₄	98.0%	N/A ^b	C₁₂H₂₃⁺(79)	C ₈ H ₁₅ ⁺ (10)	C ₇ H ₁₃ ⁺ (11)
				<u>C₁₅H₂₉⁺(77)</u>	<u>C₇H₁₃⁺(7)</u>	<u>C₈H₁₅⁺(<5)</u>
<u>Cyclopentadecane</u>	<u>C₁₅H₃₀</u>	<u>98.0%</u>	<u>N/A^b</u>	<u>C₉H₁₇⁺(<5)</u>	<u>C₁₀H₁₉⁺(<5)</u>	<u>C₁₁H₂₁⁺(<5)</u>
				<u>C₁₅H₃₀⁺(6)</u>		
<u>Nonylcyclohexane</u>	<u>C₁₅H₃₀</u>	<u>98.0%</u>	<u>N/A^b</u>	<u>C₁₅H₂₉⁺(74)</u>	<u>C₇H₁₃⁺(19)</u>	<u>C₈H₁₅⁺(<5)</u>
				<u>C₉H₁₇⁺(<5)</u>	<u>C₁₀H₁₉⁺(<5)</u>	<u>C₁₁H₂₁⁺(<5)</u>
Bicyclohexyl	C ₁₂ H ₂₂	99.0%	9.41	C₁₂H₂₁⁺(71)	C ₅ H ₁₁ ⁺ (17)	C ₅ H ₁₃ ⁺ (<5)
				C ₇ H ₁₃ ⁺ (5)	C ₈ H ₁₅ ⁺ (<5)	C₈H₁₅ C₁₂H₂₂⁺(<5)
1-Heptene	C ₇ H ₁₄	99.5%	9.34	C₇H₁₃HNO⁺(40)	C ₅ H ₉ HNO ⁺ (15)	C ₁₂ H ₂₂ ⁺ (<5)
				C ₃ H ₅ HNO ⁺ (<5)	C ₇ H ₁₄ ⁺ (<5)	C ₄ H ₇ HNO ⁺ (37)
				C₁₀H₁₉HNO⁺(51)	C ₅ H ₉ HNO ⁺ (18)	C ₆ H ₁₁ HNO ⁺ (15)
1-Decene	C ₁₀ H ₂₀	99.5%	9.42	C ₄ H ₇ HNO ⁺ (12)	C ₁₀ H ₁₉ ⁺ (<5)	C ₇ H ₁₃ HNO ⁺ (<5)
				C ₁₀ H ₂₀ ⁺ (<5)		

^a NIST chemistry web book (<http://webbook.nist.gov>)

^b N/A stands for “not available-”

Table 2. Carbon numbers and formula, means normalized sensitivities and detection limits of cycloalkanes in NO⁺ PTR-ToF-MS.

Cycloalkanes (C number)	Formula	Normalized sensitivities (ncps ppb ⁻¹)	Detection limit (ppt)	
			10s	1min
C ₁₀	C ₁₀ H ₂₀	231.3	7.20	3.04
C ₁₁	C ₁₁ H ₂₂	207.8	7.72	2.76
C ₁₂	C ₁₂ H ₂₄	223.9	7.01	2.85
C ₁₃	C ₁₃ H ₂₆	244.6	6.24	2.46
C ₁₄	C ₁₄ H ₂₈	247.9	6.22	2.40
C ₁₅	C ₁₅ H ₃₀	N/A ^a	6.67	2.54
C ₁₆	C ₁₆ H ₃₂	N/A	7.28	2.96
C ₁₇	C ₁₇ H ₃₄	N/A	7.46	3.05
C ₁₈	C ₁₈ H ₃₆	N/A	7.90	3.40
C ₁₉	C ₁₉ H ₃₈	N/A	8.21	3.61
C ₂₀	C ₂₀ H ₄₀	N/A	8.08	3.48

^a N/A stands for “not available-”. The average sensitivity of C₁₀-C₁₄ cyclic alkanes was used to predict the concentrations of cyclic alkanes with higher carbon (C₁₅-C₂₀) and bicyclic alkanes (C₁₀-C₂₀).

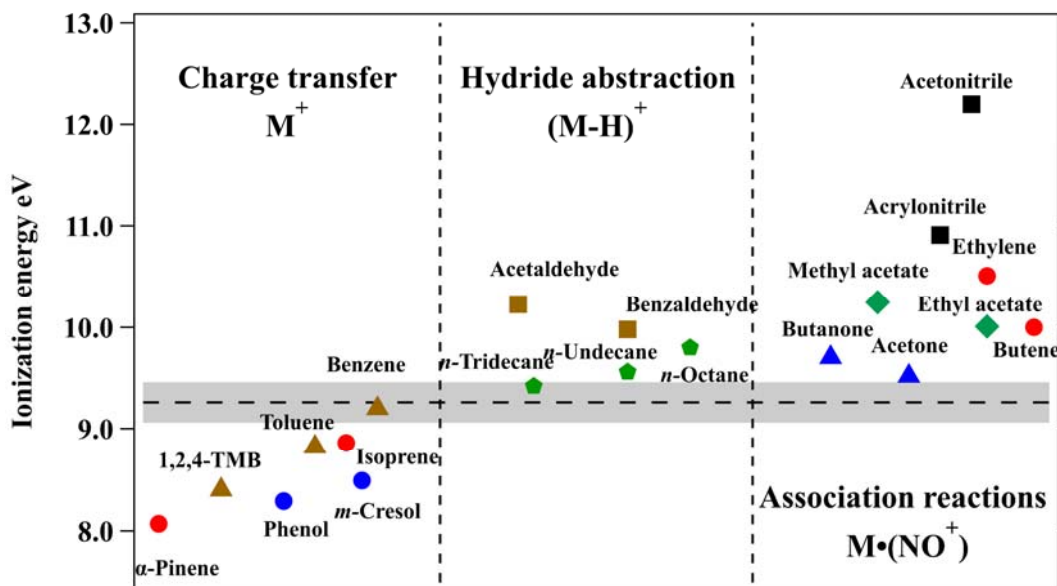


Figure 1. Ionization energy and reaction pathways with NO^+ ions of organic compounds including alkanes (green pentagon), aromatics (brown triangle), alkenes (red circle), phenolic species (blue circle), aldehydes (brown square), ketones (blue triangle), esters (green diamond), and nitrogen-containing species (black square). The ionization energy of NO (9.26 eV) is represented by the dashed line with shading representing reported uncertainty. The IE of various organic compounds are obtained in the NIST chemistry web book (<http://webbook.nist.gov>).

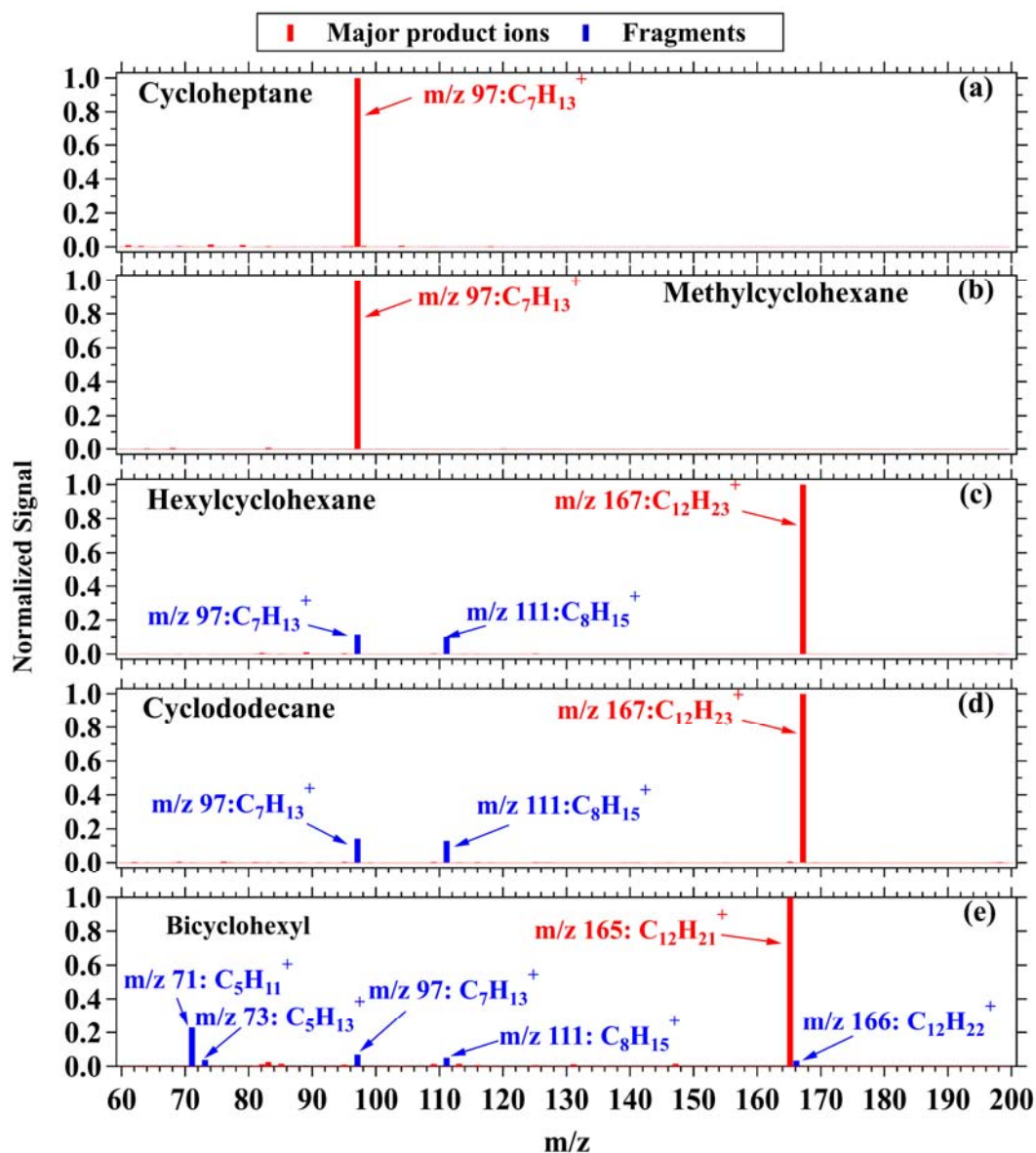


Figure 2. Mass spectra of product ions from cycloheptane (a), methylcyclohexane (b), hexylcyclohexane (c), cyclododecane (d) and bicyclohexyl (e) in NO⁺ PTR-ToF-MS. The major product ions are shown in red, and the fragments are shown in blue.

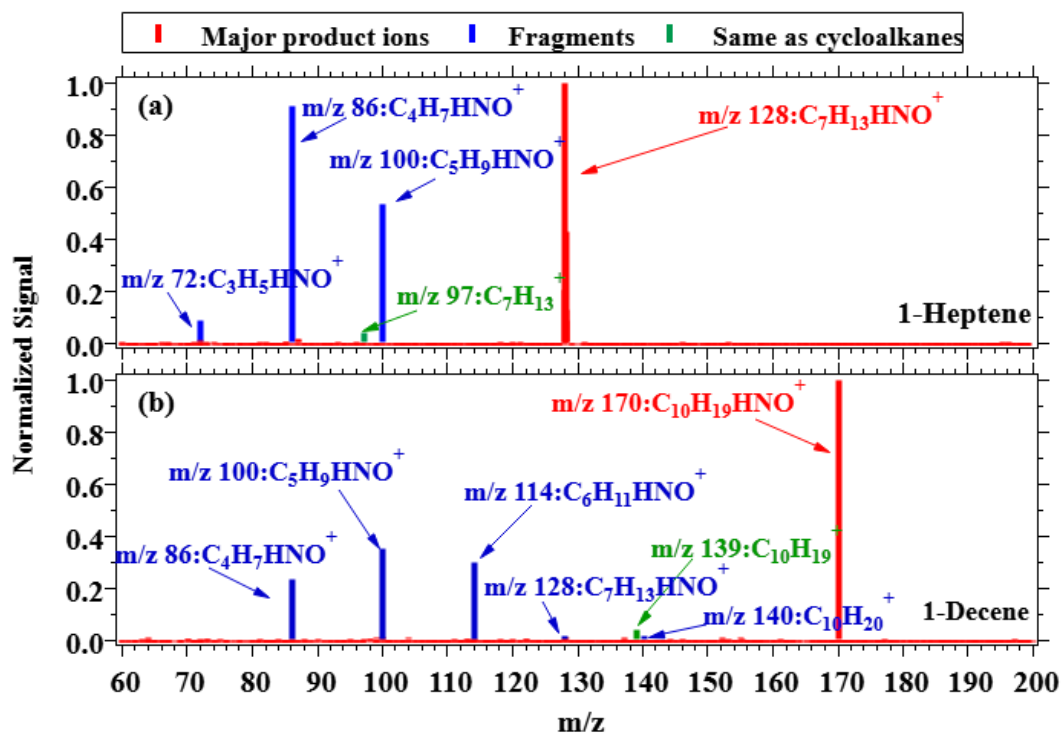


Figure 3. Mass spectra of product ions from 1-heptene (a), and 1-decene (b) with NO^+ PTR-ToF-MS. The major product ions are shown in red. The same product ions as the cycloalkanes (M-H ions) are shown in blue, and other fragments are shown in green.

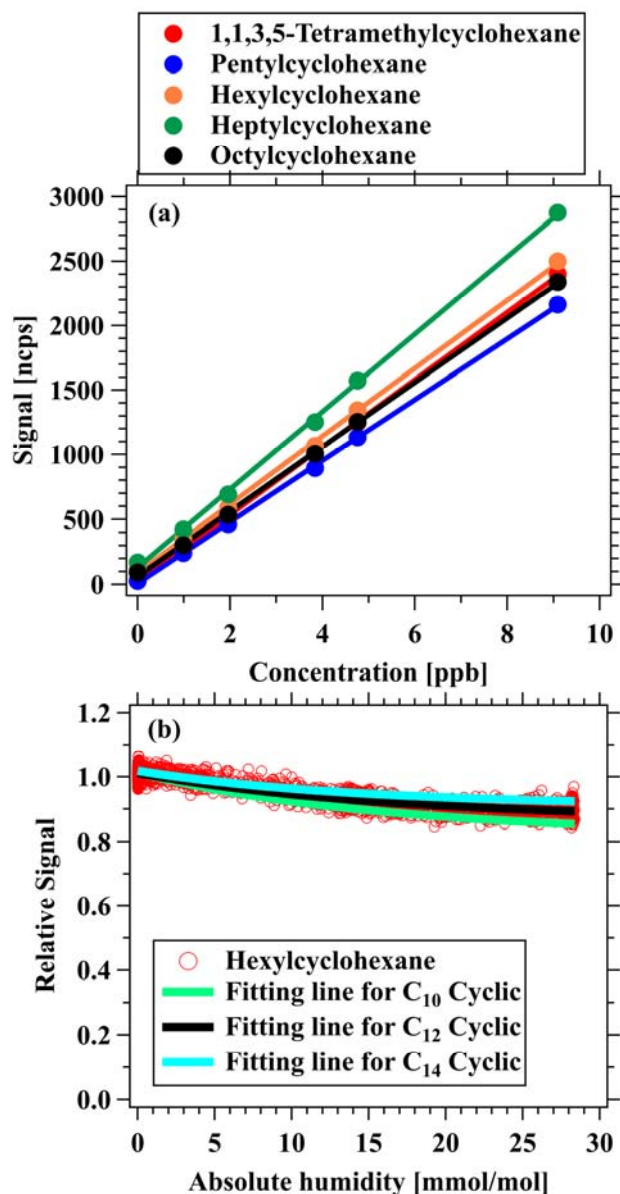


Figure 4. (a) Multipoint calibration curve for 1,1,3,5-tetramethylcyclohexane (red), pentylcyclohexane (blue), hexylcyclohexane (orange), heptylcyclohexane (green) and octylcyclohexane (black). **(b)** Humidity dependence of sensitivity for various cycloalkanes, including measurement results for hexylcyclohexane (red markers), and the fitted lines for C₁₀ cyclic alkane (green), C₁₂ cyclic alkane (black), and C₁₄ cyclic alkane (blue), with the corresponding fitted functions of $y=0.82+0.19\times\exp(-0.06x)$, $y=0.87+0.14\times\exp(-0.06x)$, and $y=0.90+0.11\times\exp(-0.07x)$, respectively.

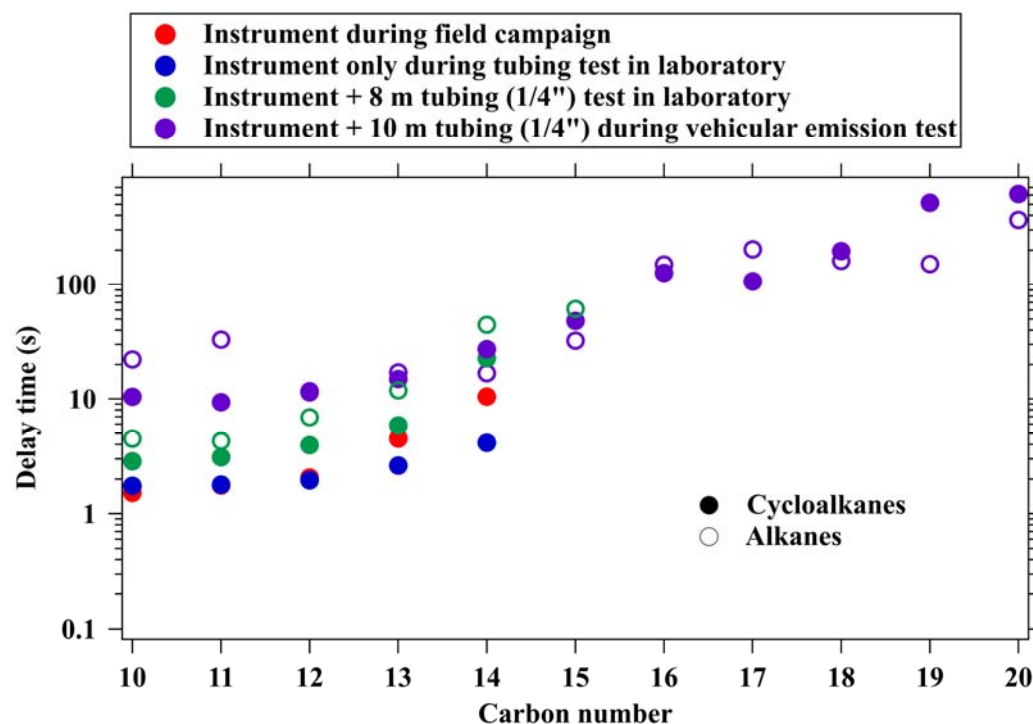


Figure 5. Delay time of cycloalkanes determined from measurements in the field, from laboratory experiments, and vehicular emissions. The delay times of alkanes from Wang et al. (2020) are also shown for comparison.

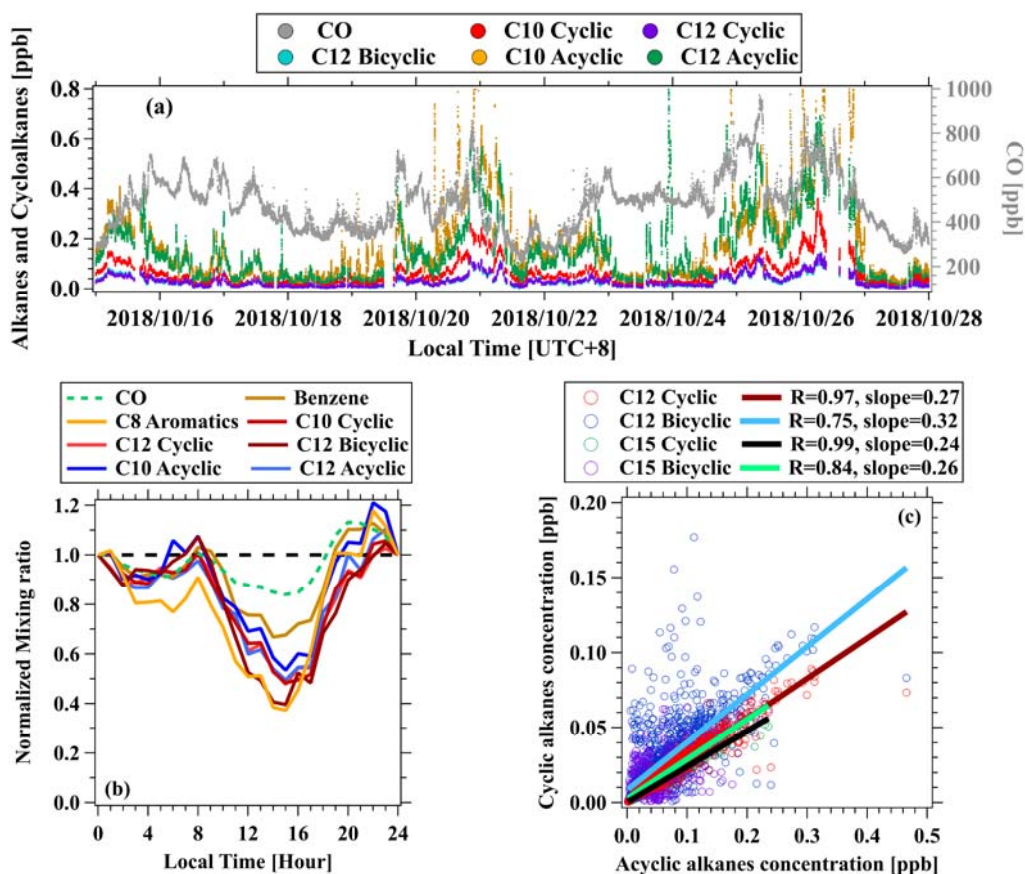


Figure 6. (a) Time series of CO, cyclic, bicyclic, and acyclic alkanes measured at the urban site in Guangzhou. **(b)** Normalized diurnal variations of CO, benzene, C₈ aromatics, C₁₀ cyclic alkanes, C₁₀ acyclic alkanes, C₁₂ cyclic alkanes, C₁₂ bicyclic alkanes and C₁₂ acyclic alkanes. The measurement data for each species is normalized to midnight concentrations. **(c)** Scatterplots of cyclic and bicyclic alkanes to acyclic alkanes with carbon atoms of 12 and 15.

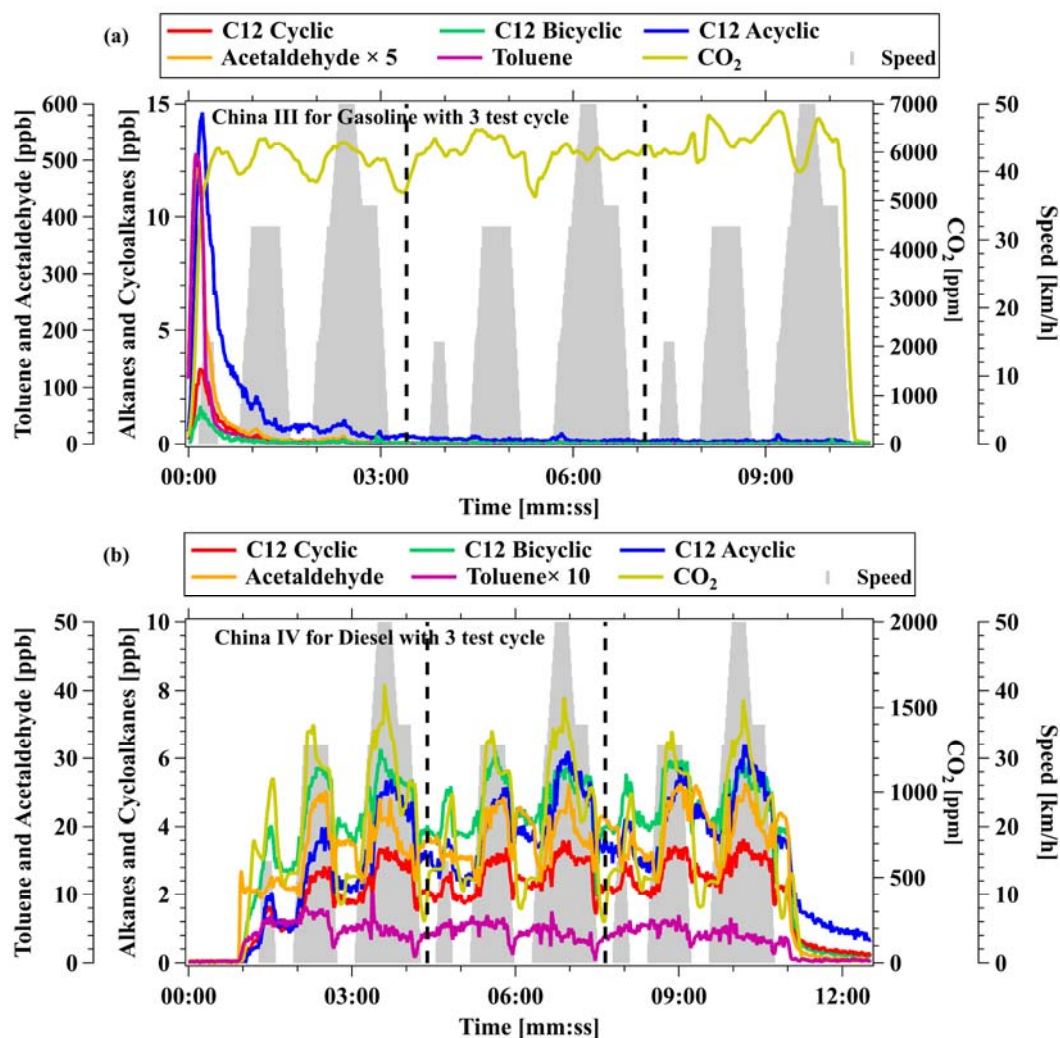
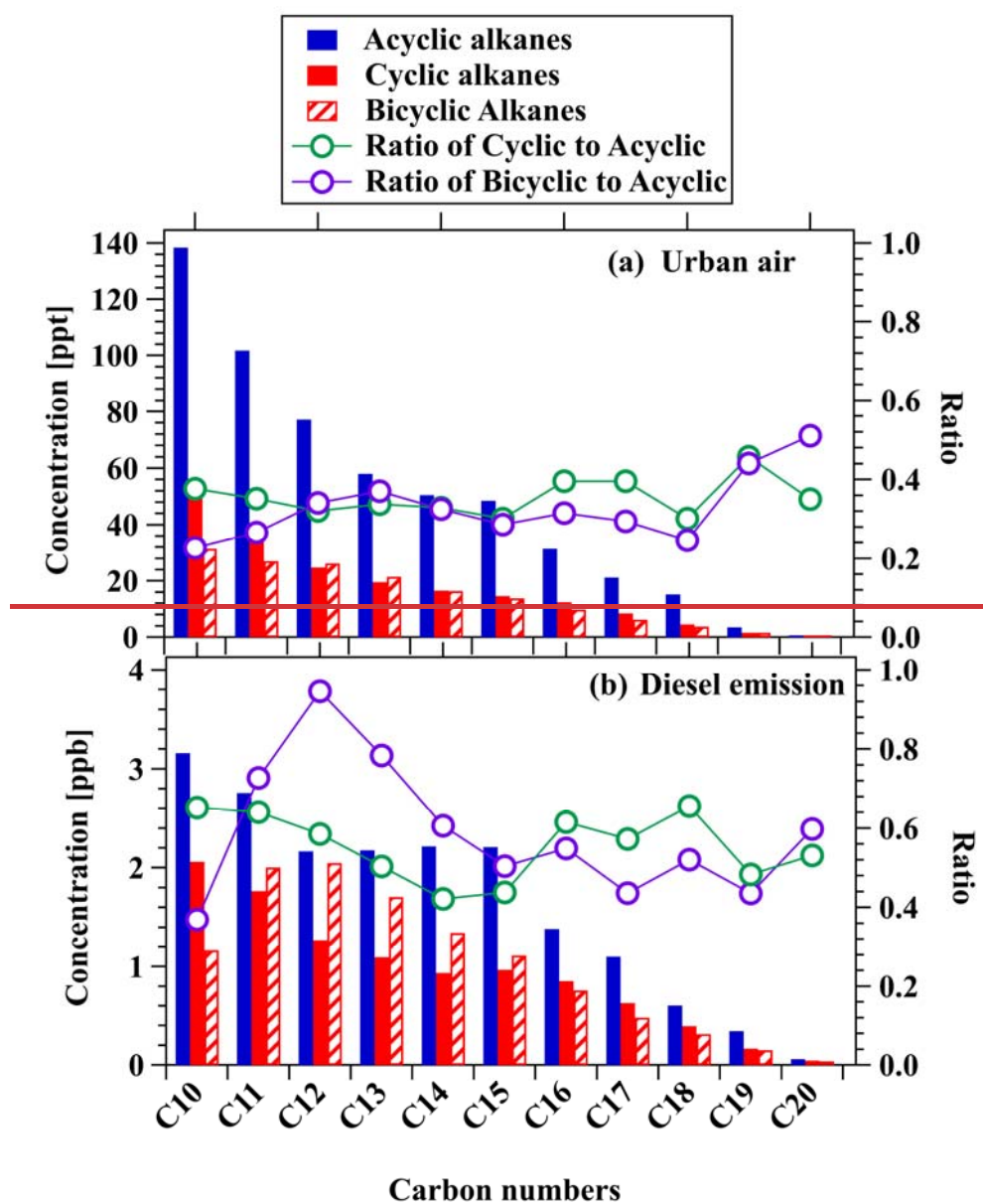


Figure 7. Concentrations of C₁₂ cyclic, bicyclic, and acyclic alkanes, acetaldehyde, toluene, and CO₂ for **(a)** a gasoline vehicle with emission standard of China III and **(b)** a diesel vehicle with emission standard of China IV. The gray shadows represent the speeds of the vehicles on the chassis dynamometer. The data of toluene and acetaldehyde were detected by NO⁺ PTR-ToF-MS.



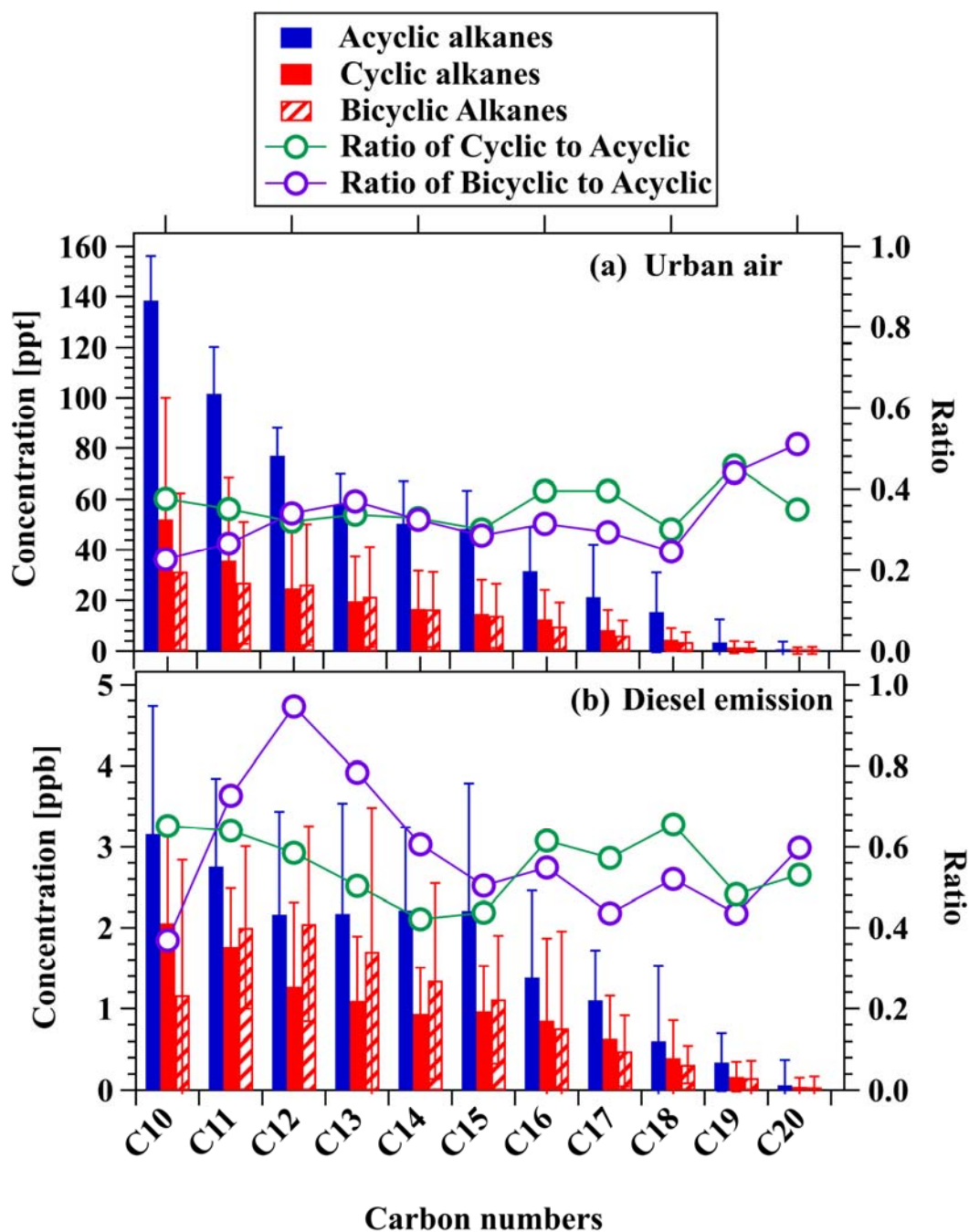
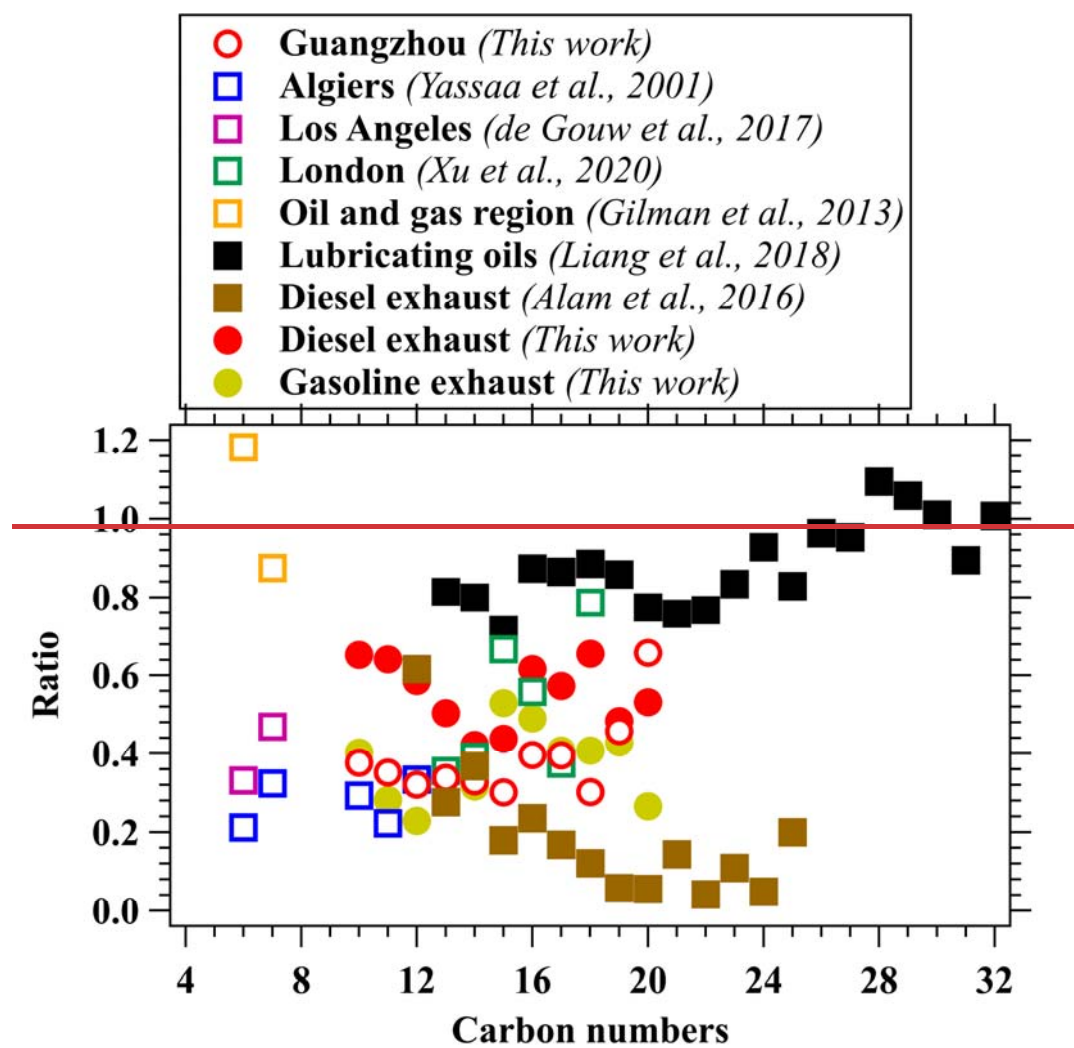


Figure 8. Mean concentrations of cyclic and bicyclic alkanes and alkanes (branched + linear) with different carbon numbers measured by NO^+ PTR-ToF-MS in the urban air (a) and diesel emissions (b). The green and purple lines with circles represent the ratios of cyclic and bicyclic alkanes to acyclic alkanes under the same carbon numbers, respectively. Error bars represent standard deviations of the concentration for the acyclic, cyclic and bicyclic alkanes.



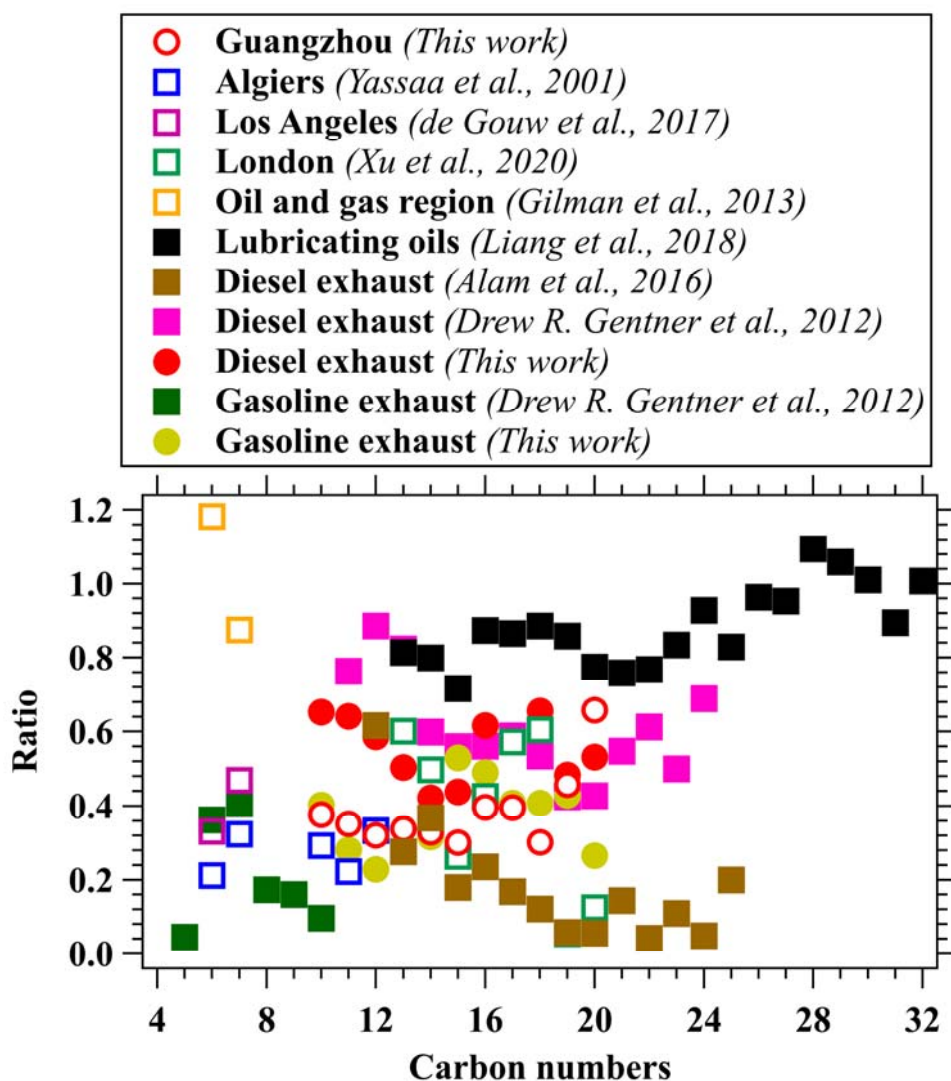


Figure 9. The concentrations ratios of cyclic alkanes to acyclic alkanes for different carbon number. Measurements in various urban areas, including Guangzhou in China, London in UK (Xu et al., 2020b), Los Angeles in US (de Gouw et al., 2017), Algiers in Algeria (Yassaa et al., 2001), and an oil and gas region in Colorado of US (Gilman et al., 2013) are also shown for comparison. Emission sources, including vehicle exhausts (Alam et al., 2016; Gentner et al., 2012) and lubricating oils (Liang et al., 2018) are also included.